

# Simulation of electrical ageing in insulating polymers using a quantitative physical model

L A Dissado<sup>1</sup> and A Thabet<sup>2</sup>

<sup>1</sup>Department of Engineering, University of Leicester, Leicester LE1 7RH, UK

<sup>2</sup>Department of Electrical Engineering, High Institute of Energy, South Valley University, Aswan, Egypt

**Abstract.** A quantitative physical model has been expressed in terms of features generic to electrical ageing. This has been used to simulate the evolution of damage structures during the electrical ageing of insulating polymers. During the main part of the ageing process isolated regions of damage were produced at a few extremely susceptible sites. However failure occurred via an accelerating filamentary damage path initiated in a region where a high energy concentration caused a number of adjoining sites to fail around the same time rather than through the connection of pre-existing damage regions.

PACS: 70, 77.84Jd, 77.22Jp

## **1. Introduction**

Polymeric insulation in service experiences electric fields well below the critical level required for failure via a deterministic runaway mechanism [1]. In this case the material should reach a field-dependent equilibrium state, but failures do occur after a period of time. Some failures may be caused by electrode protrusions, metallic inclusions, and partial discharges in gas-filled voids. These features raise the local electric field to levels at which damage may be initiated but because of the field divergence are unable to maintain its magnitude at a high enough value to cause the damage to runaway to failure. As a result a decelerating tree-like damage structure is formed [1] that will lead to failure in the short to medium term. Modern production techniques using superclean materials have almost eliminated such initiating features, but nonetheless insulation materials do breakdown in the long term often of a filamentary form without any evidence for an associated tree-like structure (see for example [2]). These failures are regarded as being due to an electric ageing process. However an unambiguous identification of the physical and chemical changes that occur in the insulating material during the period of ageing and thereby determine the extent and nature of the ageing has not yet been made [3]. A number of competing theories [4-7] exist each based on different physical mechanisms, but all predict relationships between the material life and the applied field and temperature, which give good fits to the mean (characteristic) lifetime in the distribution that characterises the statistical nature of electrical ageing [8]. This similarity means that details of the physics behind the ageing process cannot be determined through fits to experimental values of insulation lifetime however it implies that the process possesses generic features that are independent of the detailed physics of the ageing mechanism. These generic features are identified here from the life expression of the most general of the theories [5,9]. This expression will be used in our simulations with the aim of describing the damage structures produced during ageing and identifying the key generic features that determine eventual failure.

## **2. Generic features of life expression**

The starting point for our simulations is equation (1) for the insulation life ( $L$ ). This has already been shown to fit the experimental data for the characteristic life of a number of insulating polymers [5,9].

$$L = \left(\frac{h}{2kT}\right) \exp\left(\frac{G\# - CE^{4b}/2}{kT}\right) \frac{\ln\left[\{(A_q - A_o)/(A_q - A^*)\}\right]}{\cosh\left(\frac{\Delta - CE^{4b}}{2kT}\right)} \quad (1)$$

The philosophy behind equation (1) is that energy available from the electric field ( $E$ ) drives local modifications to the insulating polymer via elemental units of change. The theories [4-7] agree that the elemental units can be thought of as sections of polymer chain, and estimations in [6,10] indicate that they may occupy a volume of up to several thousand cubic nanometres. Each elemental change involves the passage of a free energy barrier by these polymer sections from the local state favoured in the absence of an electrical field to a different state made energetically more favourable in the presence of the field. The elemental changes accumulate in each locality but tend towards a local field-dependent equilibrium unless they exceed a local critical level. At this point they become irreversible in the form of cracks, crazes, and sub-micro-voids. These are more conducting than the surrounding matrix, either through long electron mean free paths or local electrical discharges, and are capable of initiating failure via a rapid extension.

The generic features of expression (1) are listed as follows.

1. An activation free energy  $G\#$  for the rate of ageing. Here,  $G\# = H\# - TS\#$ , where  $H\#$  is the activation enthalpy and  $S\#$  is the activation entropy. All the theories [4-7] contain this term.
2. An energy  $\Delta$  required to create a single local elemental modification. Only [5,7] contain this term as an explicit factor, which expresses the assumption that the initial conformation of the elemental polymer section of the polymer is favoured in the absence of the electric field.
3. A field dependent energy,  $CE^{4b}/2$  that reduces the free energy barrier and stabilises the local elemental modification that defines the ageing process. All the theories [4-7] contain a term of this form though the explicit dependence of the parameter  $C$  upon material properties varies depending upon the physical mechanism assumed to be operative in ageing. In [5]  $C$  is proportional to a product of a factor relating the local electric field including the space charge contribution to the applied field and  $(\alpha^2/Y\epsilon^4)$ , where  $\alpha$  is the local electrostriction coefficient,  $Y$  is the local value of bulk modulus, and  $\epsilon$  is the local permittivity. In [4] and [6]  $C$  is proportional to the product of  $\epsilon$  and the local volume affected by the change. This term defines the field energy that can be used to render the elemental modifications energetically more favourable.

4. A field-dependent equilibrium, defined by the fraction  $A_q$  ( $0 < A_q < 1$ ) of elemental units that are converted to a modified form at equilibrium ( $A_0$  is the fraction converted before ageing starts). Only [5,7] contains this term explicitly though its presence is implied in [4]. This term defines the thermal equilibrium between the different conformations that would exist in the absence of an irreversible change.  $A_q$  is not an independent parameter as it is defined in terms of other parameters;

$$A_q = \left[ 1 + \exp\left(\frac{\Delta - CE^{4b}}{kT}\right) \right]^{-1} \quad (2)$$

5. A critical amount of energy required for the local modifications to become irreversible given by  $NA^*\Delta$ , where  $N$  is the number of elemental units involved in this change, and  $A^*$  is the critical fraction that must change for irreversibility. Only [5,7] contains this term explicitly though its presence is implied in [4]. This term results in a field threshold as the change produced by the local field has to be sufficient to raise  $A_q$  to a value greater than  $A^*$ .

Insufficient is known about the local polymer properties to obtain values for the parameters *a-priori*. Instead values are usually obtained by fitting to experimental data and retrospective justification of their magnitude [4-6]. However it is clear that the parameters can be given a generic interpretation that is independent of their physical origin. Thus ageing requires: a) a free energy barrier to be crossed, b) energy supplied by the electric field to make a local alteration stable, c) a critical amount of local change for irreversibility. In the following we will treat the appropriate parameters as local variables with the aim of determining the relative importance of local energy concentration (proportional to  $C$  and local field) and susceptibility to ageing (dependent upon  $A^*$ ) in determining failure and failure structures.

### 3. Simulation

Insulating polymers are at most only semi-crystalline, with a spatially varying morphology. Consequently there will be a spatial variation of the model parameters, which has been suggested to be the origin of the distribution of lifetimes [8]. Our simulation will therefore treat the polymer as possessing local values of the model parameters that relate to the major generic features, selected at random from a range of values centred on the parameter value found to reproduce the characteristic value of the life distribution [8].

The polymer chosen for this study is Polyethylene Terephthallate (PET) and the mean parameter values used (Table 1) have been shown to describe well the dependence of the characteristic life as a function of dc

electric field in the temperature range [9] 110 °C to 180 °C. The simulation is realized on a 2D square grid that is taken to represent a sample 1mm thick containing no metallic protrusions, inclusions, or voids. There is an electrode at the top and bottom between which a dc potential is applied. The grid mesh has 42x40 grid-bonds and thus each bond in the mesh is 25  $\mu\text{m}$  long. Though the thickness of the simulation grid is reasonably typical of test samples the width is very small, and the edges could have a disproportionate effect upon the simulation of bulk features. In order to minimize this effect we have imposed a condition whereby the field along the edge retains the same uniform value throughout the simulation. In addition any simulation that ends upon the edge is excluded from consideration.

At the beginning of the simulation each bond of the 25  $\mu\text{m}$  mesh is in its un-failed state, which is taken to be that of a non-conducting capacitor. Each of these grid bonds is assigned a set of parameter values. In these simulations  $b$  is kept at its characteristic value as it is a feature of the ageing mechanism rather than a material property [4-6,9]. The activation enthalpy and entropy ( $H^\#$  and  $S^\#$ ) have also been kept at their characteristic value as previous derivations of the life distribution based on material inhomogeneity and extreme value statistics [8] show that there is very little spatial variation in their value. The assigned value of  $A^*$  and  $C$  have however been chosen at random from an allowed range, with each value in the range being equally probable. The ‘top-hat’ form of parameter value distribution was chosen because it is a reasonable first step approximation to a more appropriate Gaussian or Asymptotic Extreme Value [8] distribution of similar form, and thus is likely to yield the same general features of behaviour.

**Table 1.** Parameter values for the dc life [9] of PET. The unit denoted K stands for temperature in Kelvin.

Parameter	Units	CharacteristicValue
$H^\#/k$	K	17762
$S^\#$	J/K	$-9.1 \times 10^{-25}$
$\Delta/k$	K	306
$b$	--	0.389
$C/k$	$\text{K(m/MV)}^{4b}$	1.582
$A^*$	--	0.485

Since PET is a semi- crystalline polymer variations between crystalline and amorphous regions would be expected to result in a bi-modal distribution on a size scale of  $1\mu\text{m}$  or less. The mesh size of  $25\mu\text{m}$  used here lumps both amorphous and crystalline regions together and the assigned parameter value corresponding to the shortest time to failure of the lumped region, and its distribution can be expected to have lost its bi-modal character.

The range for  $A^*$  was taken to be 0.015 to 0.985, with the characteristic 0.485 as an average value. This distribution is close to the broad peaked distribution used in [8] to fit some experimental data for PET, and allows  $A^*$  to vary considerably while eliminating sites that are already damaged ( $A^*=0$ ), and sites where every elemental unit must change ( $A^*=1$ ) corresponding to a complete local re-arrangement. The chosen range covers the typical morphological features of insulating semi-crystalline polymers which possess, crystalline, amorphous, and low-density regions, and expresses their different susceptibilities to ageing, with  $A^*$  approaching zero corresponding to the most susceptible sites. Values for  $C$  were selected at random from the range 1.3 to  $1.9\text{ K(m/MV)}^{1.556}$ , and express differences in the ability of a site to concentrate energy supplied by the electric field and use it for driving the ageing reaction. This range represents a site-to-site variation of  $\pm 18.75\%$  in the field-dependent energy for any given field, and the distribution is a first approximation to the narrow peaked distribution used in [8] to obtain a best fit to the experimental data.

All grid-bonds are treated as accumulating elemental changes once the electric field is applied. This is expressed as a fraction of their local insulation life. The bond or bonds with the shortest time to failure (irreversible modification) is/are identified using equation (1) and converted to conductors, thereby changing the local fields in the whole 2D grid at that time. The amount of life lost in all the other bonds is converted to an equivalent bond-dependent value of  $A_0$  appropriate to that time. The procedure is then repeated to find the bonds with the shortest residual life. There is no restriction on the number of bonds that may reach their end of life simultaneously.

#### **4. Results and Discussion**

Results are reported from simulations using an applied field of 40 MV/m and a temperature of 110 °C. The effects of spatial variation in  $A^*$  and  $C$  are investigated independently, by varying each parameter separately from the other, which is set to its characteristic value. A number of realizations have been carried out for each of the conditions, and figure 1 shows the damage structure at failure typical of those obtained when  $A^*$  is spatially distributed. The corresponding time evolution of the damage to failure is plotted in figure 2.

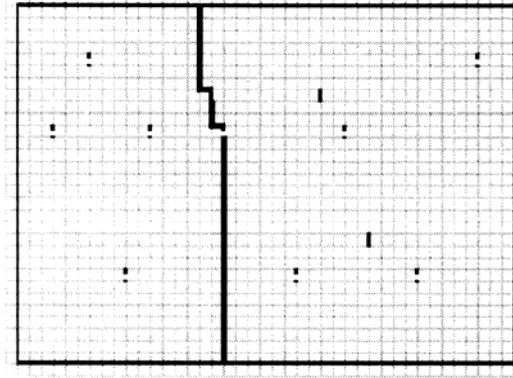


Figure 1. Damage produced by failure for  $E=40\text{MV/m}$ ,  $T = 110\text{ }^{\circ}\text{C}$  and spatial variation of  $A^*$ .

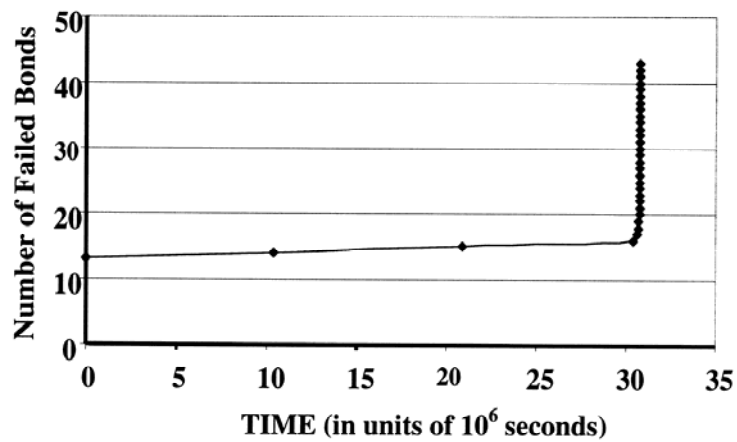


Figure 2. The evolution of damage (time in units of  $10^6$  seconds) during ageing to failure corresponding to the failure structure of Figure 1.

An inspection of the damage produced as the ageing structure evolves shows that during most of the ageing period (i.e. up to  $\sim 3 \times 10^7$  s in the example shown) only isolated bonds are damaged. Most of these remain unconnected to the breakdown path as can be seen in figure 1. Even though these bonds have small values of  $A^*$  and hence are the sites that are most susceptible to damage they were not capable of extension to cause a

sample failure. Instead sample failure was initiated by the irreversible damage of a bond in a region where the increase in local field, and hence of local energy concentration was enough to damage neighbouring bonds in a similar time i.e. in a region where a group of  $A^*$  values were similar in magnitude. The initiation therefore takes a considerable time ( $\sim 3 \times 10^7$ s in figure 2), but once one bond fails neighbours fail rapidly producing an accelerating extension of the damage that rapidly connects the two electrodes via the conducting path that defines a sample failure. Any isolated damaged bonds lying on or next to the path are absorbed into it and cause minor deviations from a straight line in the failure path. The repeat simulations showed the same pattern of behaviour though the time-to-failure of the sample differed from realization to realization. Simulations were also carried through with the range of available values for  $A^*$  reduced to 0.4 to 0.6. Again the simulations produced a small number of isolated bond-failures during the major part of the ageing period, followed by a rapidly accelerating formation of a conducting path across the simulation sample.

The failure structures obtained in these simulations are similar in form to what would be expected of a deterministic runaway process where local reinforcement of damage generation leads to a filamentary conducting path between the electrodes [1], as is the evolution of damage, as shown in figure 2. The difference here is that the onset of runaway is substantially delayed while local morphological changes reach irreversibility in a region that is suitable for runaway initiation, rather than being initiated at the most susceptible site. The key material factor determining the insulation life is not the susceptibility of individual local sites to ageing damage but the clustering of susceptible sites together such that the increase in energy concentration produced by the failure of any one of them is sufficient to fail others, leading to a self reinforcing extension of the damage. This conclusion is strengthened by the results from simulations where  $A^*$  is kept fixed and  $C$  is given a spatial variation. Here also the evolution of damage is very slow, corresponding to isolated damaged sites, until an accelerating damage path is produced that fails the sample. The damage structures are similar to that of figure 1 but have less isolated failures during ageing. Because of the similarity of these damage structures to those of figure 1 they have not been included here, however the point is illustrated in figure 3, which shows that only nine isolated bonds failed before the failure started to run away across the simulation sample, in contrast to fifteen in figure 1 as shown in figure 2.



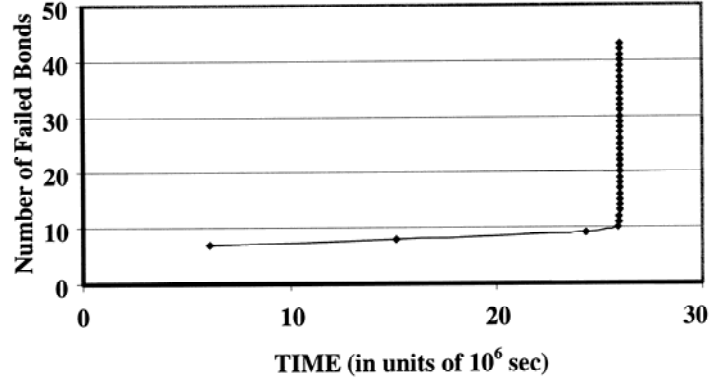


Figure 3. The evolution of damage during ageing typical of a spatial variation in parameter C.

A similar result was found for all the repeat simulations. It is probable that the reduction of isolated failures in the case of the spatial distribution of values of the parameter C is because the failure of one bond not only increases the local field but has the possibility that neighbouring bonds have a higher than average ability to concentrate energy, whereas in the case of  $A^*$  variation only the local field increase can affect the local energy concentration. A recent stochastic extension [11] of the percolation model for dielectric breakdown [12] showed similar results. They found that when the local rate of degradation extension is a strong function of the local field failures had the form of a filamentary path, otherwise clusters of degradation linked together to connect the electrodes. The proven [5,9] quantitative nature of our approach shows that energy concentration is the key factor in initiating the filamentary failure, and that failure via a percolation cluster of damage is unlikely to occur.

The simulations presented here suggest that the reason why it has proved so difficult to identify the material changes that occur during electrical ageing [3] is because only a small concentration of isolated failed regions are produced during the main part of the ageing period, and it is this damage that would be detectable as nano-voids, cracks or local conducting regions. Other regions have suffered changes but these have not reached the critical level for irreversibility and these changes would be very difficult to detect during the main period of ageing, given the typical background variation in sub-microscopic morphology. Their reversibility would also indicate local recovery if the stress were removed. The simulations also show that

material improvement should be focussed on reducing the occurrence of regions of similar sites with a greater than average susceptibility to ageing and/or energy concentration ability.

The distribution of lifetimes obtained by repeat simulations was found to fit the Weibull [1,8] failure probability ( $P_F$ ), equation (3), as shown in figure 4..

$$P_F = 1 - \exp\{-(t/\alpha)^\beta\} \quad (3)$$

Here  $\alpha$  is the characteristic life and  $\beta$  the parameter that governs the shape of the distribution with  $\beta > 1$  corresponding to a peaked distribution and  $\beta < 1$  a distribution that decreases monotonically as time,  $t$ , increases [1] (as in infantile mortalities).

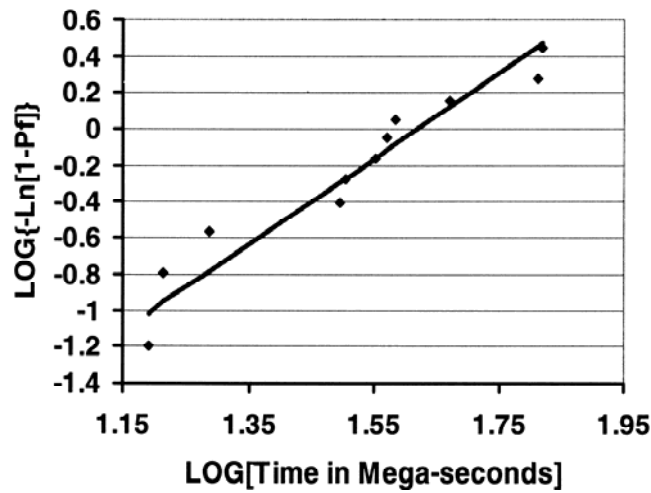


Figure 4. Probability plot of lifetimes obtained from repeat simulations. A straight line indicates a fit to equation (3)

The evaluation of the parameters  $\alpha$  and  $\beta$  from experimental data cannot be made exactly because of the limited number of samples tested. The best that can be achieved is the most likely value and the range of values between which the actual value lies with a specified level of confidence, usually 90%. In the case of PET adopted for the simulations described here it was found that the 90% confidence range for the value of  $\beta$  overlapped considerably for the various fields and temperatures investigated, with the overall average most likely value being  $\beta = 1.72$  [5] and the overall 90% confidence range giving  $0.8 < \beta < 3$ . The simulation value of  $\beta$  lies inside the 90% confidence range of the experimental results. It should also be noted that

because its value is greater than unity it corresponds to a hazard rate  $(\beta t^{\beta-1} \alpha^{-\beta})$  [1] that increases with time and hence is appropriate for an ageing process. Since our aim here was not a detailed fit to experiment but rather the investigation of the general features that the ageing models yield the distribution used for  $A^*$  is only a first approximation to the broad peaked distribution shown in [8] to give a good fit to experimental data for PET. A suitable modification of the parameter distribution can therefore be expected to bring our results closer to experiment. For example the simulation for a range of  $A^*$  between 0.4 and 0.6 reduced the value of  $\beta$  to 2.1. The characteristic life  $\alpha$  is  $4.1 \times 10^7$  second, which is substantially higher than the experimental value of  $7.4 \times 10^6$  seconds, even though the average value of  $A^*$  in the distribution is that of its fitted characteristic value in Table 1. However reduction of the range of  $A^*$  to 0.4 to 0.6 reduces the value of  $\alpha$  to  $3.2 \times 10^7$  seconds, so it is likely that a suitably modified distribution will result in a value close to experiment as in [8].

Equation (3) is an extreme value distribution [1,8] and it has usually been assumed [8] that this implied that failure is initiated at the site with the worst parameter value in the sample. The simulations however show that local sites that are the most susceptible to ageing or allow the highest local energy concentration do not initiate failure on ageing, rather it is groups of sites that can continually increase their energy concentration that initiate the failure. It is therefore not obvious that the lifetime distribution should fit a Weibull distribution, however its observation in the simulations indicates that we can still think of failure as being initiated by an extreme (worst) region. In this case though, the regions that must be regarded as the most extreme with respect to electrical ageing are those where energy concentration can continue to increase once it has started. The ageing period is then the shortest time required for polymer modifications in such a region to reach an extent where energy concentration can start to occur.

## 5. Conclusions

We have shown how the most general expression for insulation life can be given a generic form, the parameters of which can be given an interpretation that are independent of the detailed physics of the ageing mechanism. These generic parameters are: a) the local susceptibility to modification, b) local energy concentration, and c) local activation free energies for reversible elemental changes. In this form the life

expression includes a range of theories as sub-sets, and the parameters can be determined as appropriate to the ageing conditions and the system.

Simulations made using the general expression with the parameters varying spatially yield failure structure with the form of a single filamentary path, with no branching on a size scale greater than 25  $\mu\text{m}$ . The time evolution of the damage during ageing is similar to a deterministic runaway process with a much delayed onset during which isolated regions of damage occur, with failure being initiated when sufficient morphological change is accumulated in a region that has the ability to continually increase the local energy concentration.

The lifetime distribution resulting from the simulations fits the Weibull distribution with a shape parameter that is appropriate to an ageing process (i.e. greater than unity) lying within the 90% confidence limits of the experimental value. The weakest link in the sample appropriate to this form of distribution is the region that can continually increase the local energy, rather than the region most susceptible to local damage.

## Acknowledgements

A.Thabet was supported throughout this work by a grant from the Missions Department of The Egyptian Ministry of Higher Education.

## References

- [1] Dissado L A and Fothergill J C, 1992 *Electrical Degradation and Breakdown in Polymers*, (P. Peregrinus Press for IEE, London)
- [2] Flandin L, Vouyovitch L, Beroual A, Bessede J-L, and Alberola N D, 2005, *J.Phys.D: Appl. Phys.*, **38**, 144-55
- [3] Markey L and Stevens G C, 2003, *J.Phys.D: Appl.Phys.*, **36**, 2569-83
- [4] Jones J P, Llewellyn J P, and Lewis T J, 2005, *IEEE Trans.Diel. & EI.*, **12**, 951-66
- [5] Dissado L A, Mazzanti G, and Montanari.G C , 1997, *IEEE Trans. Diel. & EI.*, **4**, 496-506
- [6] Crine J-P, 2005, *IEEE Trans.Diel. & E.I.*, **12**, 1089-107
- [7] Mazzanti G, Montanari G C, and Dissado L A, 2005, *IEEE Trans Diel. & EI.*, **12**, 876-90
- [8] Dissado L A, 2002, *IEEE Trans.Diel. & E.I.*, **9**, 860-75
- [9] Mazzanti G, and Montanari.G C and Dissado L A , 1999, *IEEE Trans. Diel.& EI*, **6**, 864-75

- [10] Dissado L A, Mazzanti G, and Montanari G C, 2001, *IEEE Trans. Dielect. & El.* **8**, 959-65
- [11] Wu K., and Cheng Y., J. 2007, *Appl. Phys.*, **101**, paper 064113
- [12] Wu K, Dissado L A, and Okamoto T, 2004, *Appl.Phys.Lett.*, **85**, 4454-56,

**Table 1.** Parameter values for the dc life [9] of PET

Parameter	Units	CharacteristicValue
H#/k	K	17762
S#	J/K	$-9.1 \times 10^{-25}$
$\Delta/k$	K	306
b	--	0.389
C/k	$K(m/MV)^{4b}$	1.582
A*	--	0.485

#### LIST OF FIGURE CAPTIONS

Figure 1. Damage produced by failure for  $E=40\text{MV/m}$ ,  $T = 110\text{ }^{\circ}\text{C}$  and spatial variation of  $A^*$ .

Figure 2. The evolution of damage (time in units of  $10^6$  seconds) during ageing to failure corresponding to the failure structure of Figure 1.

Figure 3. The evolution of damage during ageing typical of a spatial variation in parameter  $C$ .

Figure 4. Probability plot of lifetimes from repeat simulations. A straight line indicates a fit to equation (3).